Antiferromagnetic ϕ^4 model. I. The mean-field solution

Vincenzo Branchina*
Laboratory of Theoretical Physics, Louis Pasteur University, 3 rue de l'Université 67087 Strasbourg, Cedex, France

Hervè Mohrbach†
Laboratory of Theoretical Physics, Louis Pasteur University, 3 rue de l'Université 67087 Strasbourg, Cedex, France and LPLI-Institut de Physique, F-57070 Metz, France

Janos Polonyi‡
Laboratory of Theoretical Physics, Louis Pasteur University, 3 rue de l'Université 67087 Strasbourg, Cedex, France and Department of Atomic Physics, L. Eötvös University, Puskin u. 5-7 1088 Budapest, Hungary
(Received 16 September 1998; published 22 July 1999)

Certain higher dimensional operators of the Lagrangian may render the vacuum inhomogeneous. A rather rich phase structure of the ϕ^4 scalar model in four dimensions is presented by means of the mean-field approximation. One finds para-, ferro-, ferri-, and antiferromagnetic phases and commensurate-incommensurate transitions. There are several particles described by the same quantum field in a manner similar to the species doubling of the lattice fermions. It is pointed out that chiral bosons can be introduced in the lattice regularized theory. [S0556-2821(99)04614-7]

PACS number(s): 03.70.+k, 11.30.Cp, 11.30.Qc

I. INTRODUCTION

Only renormalizable quantum field theory models are considered in particle physics. This was explained traditionally by inspecting the UV divergences generated by the operators in the framework of the perturbation expansion in a homogeneous background field. The nonrenormalizable theories were rejected due to the need of infinitely many coupling constants. This argument has been further developed in recent decades. First came the realization that what really matters in particle physics are not the true UV divergences, because we do not have a complete knowledge of the theory of everything and consequently we work with effective theories. The characterization of the renormalizable operators was modified by looking into their importance at low energies. In particular the equivalence of the renormalizability of an operator with its relevance at the UV fixed point has been established [1]. Nonrenormalizable operators are excluded because they do not change the universality class; i.e., their influence on the dynamics decreases as we move away from the UV scaling regime towards the physical energy scales.

There are different mechanisms which nevertheless may turn a coupling constant which is found irrelevant in the usual treatment into an important parameter of the theory.

Loop corrections. Once the anomalous dimension is taken into account in the power counting argument [2] new relevant operators at the UV fixed point can be generated. The physical picture of the strong coupling massless QED vacuum [3] which suggested this natural generalization of the power counting method is based on the observation that the positronium may acquire a negative energy and collapse onto the size of the cutoff for $e=O(1)$. The condensate of these bound states breaks the chiral symmetry and the IR features of the resulting vacuum are modified when compared to the perturbative ones.

Multiple fixed points. Starting from the theory of everything a unique renormalized trajectory describes the composite models, grand unification, electroweak theory, QCD, QED, condensed matter physics, and solid state physics which appear as different ''scaling islands'' in the coupling constants space. One operator which is irrelevant in the vicinity of one such fixed point may turn to be relevant around another one [4].

Tree-level effects. The power counting argument traces down the influence of the loop corrections to the scaling laws. The tree level effects of certain operators might be much more complicated in relating different length scales and they may generate new important coupling constants which defy the classification based on a perturbative implementation of the Wilson-Kadanoff blocking procedure [5]. The cutoff is usually ignored in the tree-level solution though it is actually present in any consistent regularization of the path integral. When the important configurations, the saddle points, have length scales close to the cutoff these tree-level cutoff effects become more important [6]. In fact, if the semiclassical vacuum is nonhomogeneous the successive elimination of the degrees of freedom in the blocking procedure should be performed in the semiclassical approximation. The nontrivial saddle points generate new contributions to the scaling laws [7].

The surprisingly strong tree-level effects of the nonhomogeneous saddle points raise the following issue. The usefulness of the ferromagnetic condensate in mass generation has long been been recognized in particle physics [8]. The vacuum is a coherent state of particles with zero momentum. What happens if particles with nonvanishing momentum form a condensate? A close similarity can be found in the

*Email address: branchina@crnvax.in2p3.fr
†Email address: mohrbach@crnvax.in2p3.fr
‡Email address: polonyi@fresnel.u-strasbg.fr

charge or spin density wave phases of solids [9]. The emergence of these states from the normal ground state is a highly involved dynamical nonequilibrium problem. Here we are interested in the properties of the static modulated phase only.

The field expectation value in this vacuum is a nontrivial function of the space-time coordinates with a characteristic length given by the inverse of the typical momentum of the particles in the coherent state.

An oscillating saddle point configuration is formally similar to the Nèel state of the antiferromagnetic Ising model, the ground state of solids or the charge density wave state. Such a formal similarity leads to far reaching analogies between solid state physics and the phenomenology of this condensate. The nonvanishing momentum of the condensed particles extends the symmetry breaking from the internal symmetries to the external ones. The result is the dynamical breakdown of the space-time symmetries. It is well known that the ground state of the translational invariant Hamiltonian for photons, electrons and massive positively charged ions is not translational invariant for certain densities (solid state crystals). Due to the observed homogeneity of the space-time in the particle reactions the absence of the dynamical breakdown of the external symmetries was always assumed [10], or taken for granted in high energy physics.

In this paper we will consider the case of a single component self interacting scalar field theory in the presence of higher derivative terms. The semiclassical solution of our model reveals the possibility of breaking the space-time symmetries at the cutoff scale in a manner which is compatible with the homogeneity of the space-time at finite observational scales. The spontaneous breakdown of the internal symmetries is widely accepted and used in quantum field theories. The saddle point approximation which is based on the construction of a condensate in the vacuum can be used without difficulties in exploring the possibility of the spontaneous breakdown of external symmetries, too. In this case the condensate is obviously inhomogeneous. This inhomogeneity amounts to a periodic structure in our case. The apparence of an elementary cell repeated periodically in the vacuum manifests itself in the possibility of exchanging nonvanishing momentum between the propagating particles and the particles condensed in the vacuum and in the presence of several branches in the dispersion relation, such as the acoustic and optical phonons in the solid state crystals. The vacuum of the model considered in this paper consists of a condensate of particles with a given momentum, $p^\mu = P^\mu$. Thus the inhomogeneity of the vacuum leads to the nonconservation of the momentum, $p^\mu \to p^\mu \pm P^\mu$. We constrain the external symmetry by allowing those translations only which bring one elementary cell into another. The momentum defined by this subgroup of the original external symmetry group, $p^\mu_{phys} = p^\mu \bmod(P^\mu)$, is the analogous of the Bloch momentum in solid state physics and it is obviously conserved. The different branches of the dispersion relation are interpreted as different ''flavor'' states of the elementary excitations, the particles of the model. The umklapp process, where a momentum $\pm P^\mu$ is exchanged with the vacuum is then a ''flavor'' changing reaction. Thus the momentum nonconservation is traded into a ''flavor'' nonconserving dynamics where the particles in a given ''flavor'' state propagate in a homogeneous vacuum. When the momentum P^μ diverges then the space-time structure of the ''flavor'' changing processes remain unresolved for the low (physical) momentum observables.

In the lattice regularized version of our model we find the usual phases of solid state physics which belong to the para-, ferro-, ferri-, or antiferromagnetic vacuum. This rich phase structure is due to the presence of more than next neighbor couplings. In this case the dispersion relation (the quadratic part of the action at vanishing field) has two mimima at $p^\mu = 0$ and at $p^\mu = P^\mu = \pi/a$. The ferromagnetic or antiferromagnetic vacua occur when the first or the second minimum become negative. Having taken into account the condensation of the instable modes, the two minima of the new dispersion relation correspond to elementary excitations which allow us to identify two particles described by the same quantum field.

The unusual features of the model can be traced back to the fact that the condensate and the dynamical symmetry breaking are driven by the kinetic rather than the potential energy terms of the action. It has already been remarked that the kinetic energy becomes dominant in high temperature QCD and leads to the dynamical breakdown of the fundamental group symmetry in high energy processes [11]. This time the kinetic energy drives the formation of the nontrivial elementary cells in the ground state which break the space-time inversion symmetries and introduce a nontrivial length scale in the vacuum.

Here we consider the theory in the mean-field approximation. The organization of the paper is the following. In Sec. II we introduce our higher derivative Φ^4 scalar model. The tree level phase structure of this model in dimension $d \leqslant 4$ is presented in Sec. III. A more detailed analysis in the vicinity of the simplest antiferromagnetic phase of $d=4$ is performed in Sec. IV. The elementary excitations are identified by the help of the free propagator in Sec. V. The symmetry aspects of the phase diagram and the interpretation of the different particle modes of the system is the subject of Sec. VI. Finally, Sec. VII is for the conclusions.

II. HIGHER DERIVATIVE SCALAR MODEL

To study the impact of higher derivative terms in the case of the single component scalar model we choose the following action:

$$S[\Phi(x)] = \int d^d x \left\{ \frac{1}{2} \partial_\mu \Phi(x) \mathcal{K}\left(\frac{(2\pi)^2}{\Lambda^2} \Box \right) \partial_\mu \Phi(x) + \frac{m^2}{2} \Phi^2(x) + \frac{\lambda}{4} \Phi^4(x) \right\}, \tag{1}$$

where

$$\mathcal{K}(z) = 1 + c_2 z + c_4 z^2. \tag{2}$$

The dimension of the higher derivative terms is taken into account by the introduction of the scale parameter Λ.

Models with higher order derivative terms have already been considered recently [12–15]. We suppose first that the vacuum is homogeneous, $\langle\Phi(x)\rangle=\text{const}$. The quantum fluctuations are then plane waves with the eigenvalues

$$G^{-1}(p^2)=m^2+p^2-c_2(2\pi)^2\frac{p^4}{\Lambda^2}+c_4(2\pi)^4\frac{p^6}{\Lambda^4} \quad (3)$$

for the second functional derivative of the action. Modes with negative $G^{-1}(p^2)$ are unstable and generate a condensate. When $m^2<0$ and $c_j=0$ we have a ferromagnetic instability. After filling up the most unstable mode $p=0$, the system stabilizes itself and the only change in the interaction is the apparence of a three particle vertex which describes the processes where a particle is exchanged with the condensate. If $G^{-1}(p^2)$ develops a second minimum at $p\neq 0$, new particles appear in the system. When c_2 becomes large (and for simplicity we limit ourselves to consider the case $m^2=0$) an instability shows up for

$$\frac{c_2}{2c_4}-\sqrt{\frac{c_2^2-4c_4}{4c_4^2}}<(2\pi)^2\frac{p^2}{\Lambda^2}<\frac{c_2}{2c_4}+\sqrt{\frac{c_2^2-4c_4}{4c_4^2}}. \quad (4)$$

Thus a condensate of particles with nonvanishing momenta is formed. The filling of this condensate by the most unstable mode, $p_{cond}^2=c_2\Lambda^2/2(2\pi)^2c_4$, modifies the interaction between the plane wave modes in a rather complicated manner and particles with different momenta may appear in the stable condensate. It is reasonable to expect that the Fourier transform of the field expectation value is peaked around $p^2=p_{cond}^2$. Its spread is a measure of the strength of the interaction within the condensate. Notice that the action is bounded from below for $\lambda>0$ because $S\to\infty$ either when $p^2\to\infty$ or when the amplitude of the oscillations tends to infinity.

We will explore the dynamics of the effective theory (1) in the mean-field approximation. The first step will be the determination of the phase structure. The spectrum of the free quantum fluctuations will be studied later.

III. THE MEAN-FIELD PHASE STRUCTURE

In this section we classify the different phases of the scalar theory (1) at the tree level. We identify the order parameter with the condensate, $\langle\Phi(x)\rangle$, which is a nontrivial function whose Fourier transform is

$$\tilde{\Phi}_{vac}(p)=\int d^dx e^{ipx}\langle\Phi(x)\rangle. \quad (5)$$

The ferromagnetic condensate is obtained for $\tilde{\Phi}_{vac}(p)=\Phi_0\delta^{(d)}(p)$. For an antiferromagnetic condensate the function $\tilde{\Phi}(p)$ has a peak at $p\approx p_{min}$. One may also have the ferrimagnetic phase where $\tilde{\Phi}_{vac}(p)$ displays two peaks, one at $p=0$ and another at $p=p_{min}\neq 0$. When a consistent cutoff like the lattice regulator is used, there are two length scales in the antiferromagnetic vacuum, the periodic length of the condensate and the regulator itself. The phase structure is amazingly rich in this case due to the commensurate-incommensurate phase transitions. We begin our investigation by looking for the lowest action solution of the equation of motion for Eq. (1).

A. $d=1$

We have solved numerically the finite difference equation in two different regimes, $\Lambda^{-1}\gg a$ and $\Lambda^{-1}\approx a$, where a is the step size (regulator) of the equation.

The continuum theory, $\Lambda^{-1}\gg a$. The removal of the cutoff a is trivial for the tree level classical equation and one finds the solution of the differential equation as $a\to 0$. In order to find the lowest action solution we considered the configurations which yield finite action density,

$$\epsilon=\frac{1}{T}\int_0^T dx\left\{\frac{1}{2}\partial\Phi(x)\left[1+c_2\frac{(2\pi)^2}{\Lambda^2}\Box+c_4\frac{(2\pi)^4}{\Lambda^4}\Box^2\right]\partial\Phi(x)+\frac{m^2}{2}\Phi^2(x)+\frac{\lambda}{4}\Phi^4(x)\right\}. \quad (6)$$

The solutions of the variational equation are not constant since $\epsilon(0)>\epsilon(p_{cond}^2)$. At the same time the Φ^4 potential energy keeps $|\Phi(x)|$ bounded. Thus we conjecture that all solutions with finite action density are periodic and we impose periodic boundary conditions on the field, $\Phi(x)=\Phi(x+T)$. The minimization of the action density with respect to $\Phi(x)$ and T indeed leds to periodic solutions, one of them is depicted in Fig. 1(a). It was checked by increasing the volume T that the minimal action configuration remains periodic.

This result can be compared with the a variational approach where the form

$$\Phi(x)=A\sin\omega x \quad (7)$$

is assumed. The minimization of the action density with $T=2\pi/\omega$ yields

$$\omega^2=\frac{c_2\Lambda^2}{3(2\pi)^2c_4}\left(1+\sqrt{1-\frac{3c_4}{c_2^2}}\right), \quad (8)$$

and

$$\epsilon=-\frac{3\lambda A^4}{32}. \quad (9)$$

One can see that the periodicity length is determined by the c_j and the amplitude is controled by the term ϕ^4. By choosing for example $c_2(2\pi)^2=1$, $c_4(2\pi)^4=0.1$, $m^2=$

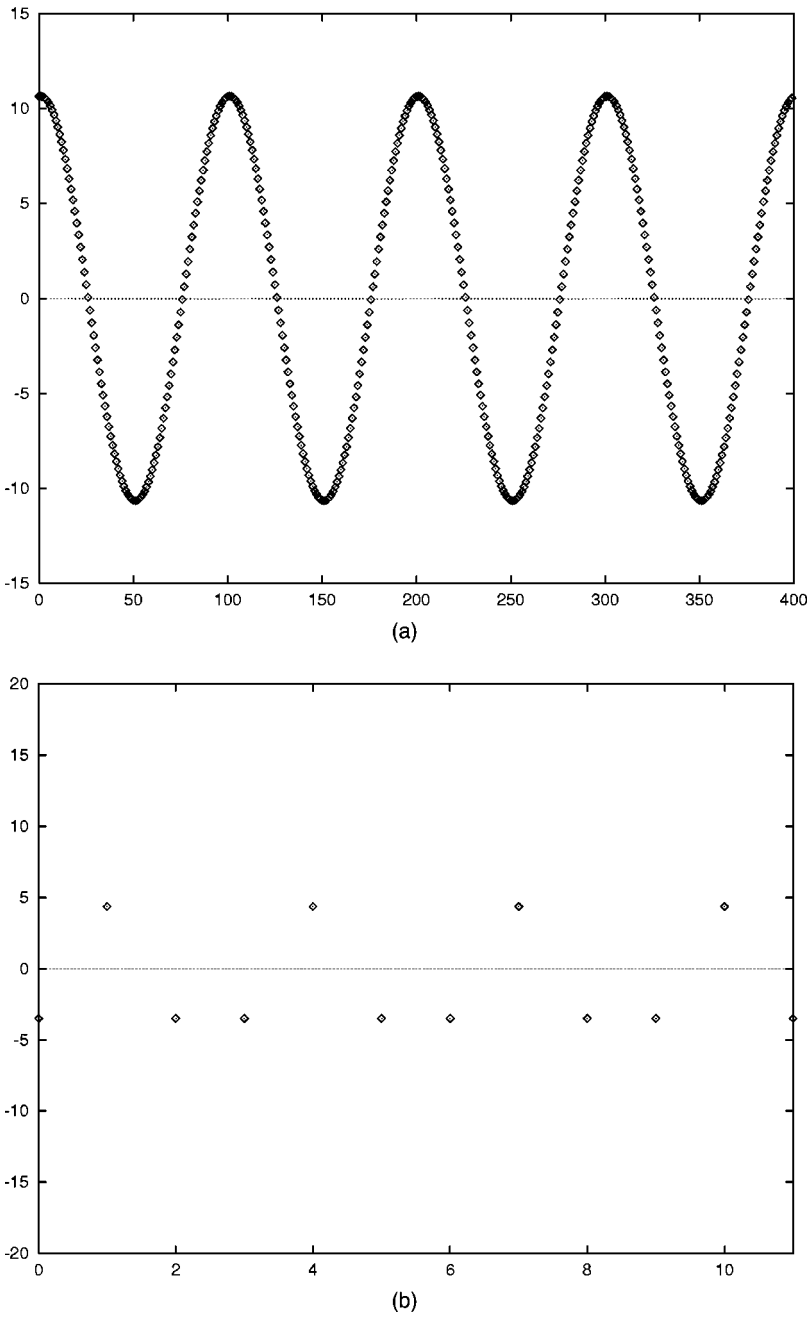

FIG. 1. Field configuration in function of x which minimizes of the action density with periodic boundary condition in $d=1$ dimension. (a) Continuum theory. (b) The vacuum of the phase (1,3) in lattice regularization.

$-0.1\Lambda^2$ and $\lambda=0.1\Lambda^3$, these two methods give $A_{num}=10.65\Lambda^{-1/2}$, $A_{var}=10.59\Lambda^{-1/2}$, $\epsilon_{num}=-120.75\Lambda$ and $\epsilon_{var}=-117.94\Lambda$.

Lattice regulated model, $\Lambda^{-1}\approx a$. The periodicity length, $l=O(p_{cond}^{-1})$, of the solution of the continuous differential equation is a ''floating,'' analytical expression of the coupling constants. This may change when finite difference equations are considered. In fact, the periodicity length of the condensate may be incommensurate [16] with the numerical discretization of the differential equation. l and a are commensurate and belong to the class (M,N) when $Ml=Na$, M and N being relative primes. In this case l locks in as a function of the coupling constants and creates a devil's staircase. A similar phenomenon was analyzed for models where the kinetic energy is quadratic but has minimum at nonvanishing momenta [17]. One can easily find the simple commensurate phases, $M=1$, N not too large, cf. Fig. 2. The high (M,N) commensurate points are presumably washed together with the incommensurate regions when the quantum fluctuations are taken into account.

We will study the particle content of the simplest antiferromagnetic phase, $(M,N)=(1,2)$ in the next section. The generalization of our method for the higher commensurate theories is possible though complicated. The spectrum of the elementary excitations of the incommensurate theories is rather involved and qualitatively different [18].

The phases $(1,N)$ with odd N are of ferrimagnetic type. This is because there are an odd number of lattice field variables within a period which in general do not add up to zero, cf. Fig. 1(b).

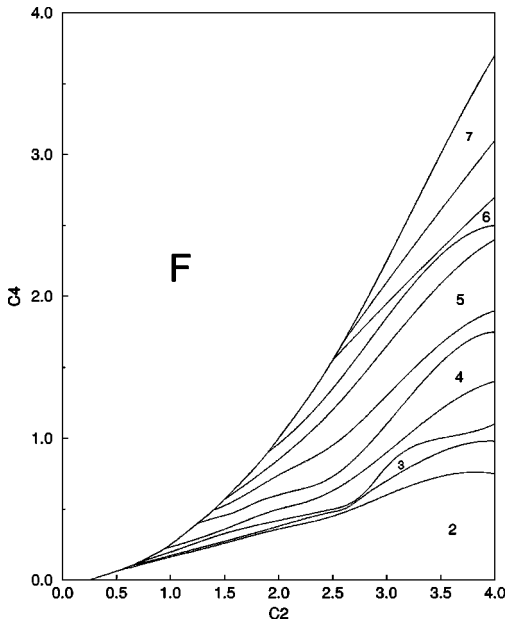

FIG. 2. The phase diagram for the lattice regularized model in $d=1$. F stands for the ferromagnetic phase and the numbers denote the parameter N of the antiferromagnetic phase $(1,N)$.

The complex phase structure of the lattice theory should be present in any other regularization as well when the regulator is introduced in a consistent manner at the tree level. One may take the sharp momentum space cutoff, as an example. Its implementation on the tree level leads to the acceptance of field configurations as possible saddle points whose Fourier components are vanishing for momenta beyond the cutoff. We believe that the solutions of the Euler-Lagrange equations which satisfy such a constraint display similar commensurate-incommensurate transitions though the details of the phase diagram may differ.

B. $d=2,3,4$

For $d>1$ the staggered order generated by c_2 is more complicated. This is due to the fact that the kinetic energy of the continuum theory is $O(d)$ invariant and the most unstable modes at the minimum of the dispersion relation are found on a S_{d-1} sphere. The minima of the dispersion relation should form a discrete set of points in the restricted Brillouin zone in order to have particle like excitations. The degenerate modes on this sphere may achieve this by creating a complicated dynamical $O(d)$ symmetry breaking pattern. The staggered antiferromagnetic order can be realized in d_{AF} dimensions, $0\leqslant d_{AF}\leqslant d$. For the cases $d_{AF}=d$, $d-1$ and $d_{AF}<d-1$ we will use respectively the names relativistic, nonrelativistic and anisotropic vacuum.

Continuum theory, $\Lambda^{-1}\gg a$. We found the local minima of the action density corresponding to the relativistic and the nonrelativistic vacuum in $d=2$ as depicted in Fig. 3. The latter is the absolute minimum. Inspired by the numerical results we have tried the following ansatz:

$$\Phi_{rel}(x,y)=A\sin\omega x\sin\omega y, \tag{10}$$

and

$$\Phi_{nrel}(x,y)=A\sin\omega x. \tag{11}$$

The variational method gives acceptable but less accurate result than in the one dimensional case for $\Phi_{rel}(x,y)$ due to the tree-level interactions which split the degeneracy of the condensate at $|p|=p_{cond}$. The highly nontrivial effect of such a deformation of the saddle point on the elementary excitation will be investigated below.

The issue of the $O(d)$ symmetry breaking pattern can be better studied in lattice regularization where the regulator is explicit already at the tree level.

Lattice regulated model, $\Lambda^{-1}\approx a$. The lattice regulated action in $d>1$ dimensions written in terms of the dimensionless variables x^μ, $\varphi=a^{d/2-1}\Phi$, $m_L^2=m^2a^2$ and the unit vectors $(e_\mu)^\nu=\delta_{\mu\nu}$ is

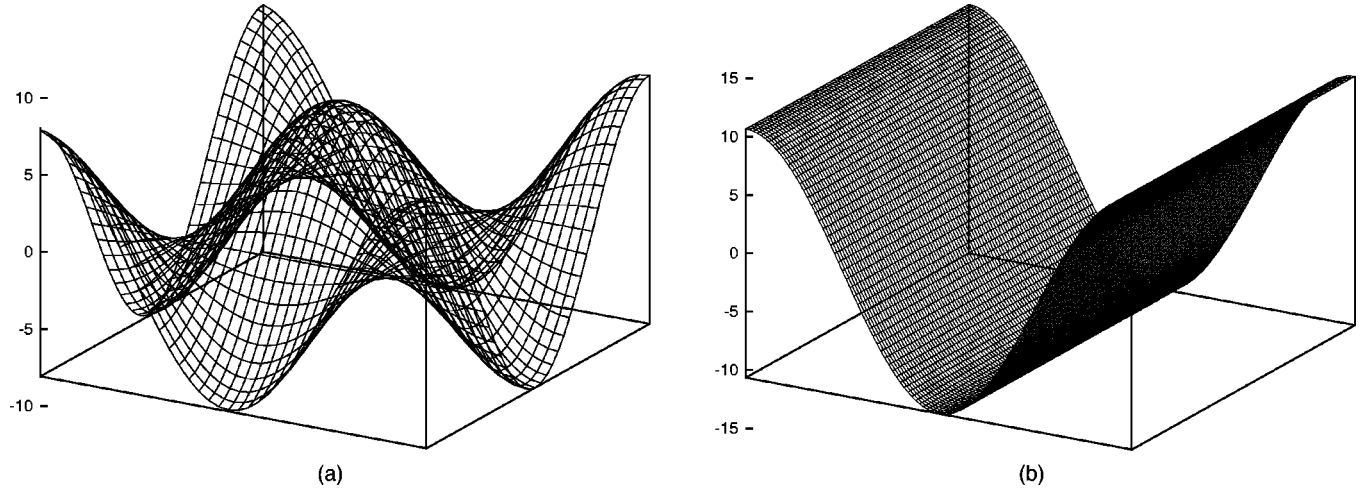

FIG. 3. The elementary cell of the antiferromagnetic vacuum configurations in the continuum as the functions of x^μ in $d=2$. (a) Relativistic vacuum, a local minimum. (b) The nonrelativistic vacuum, the absolute minimum.

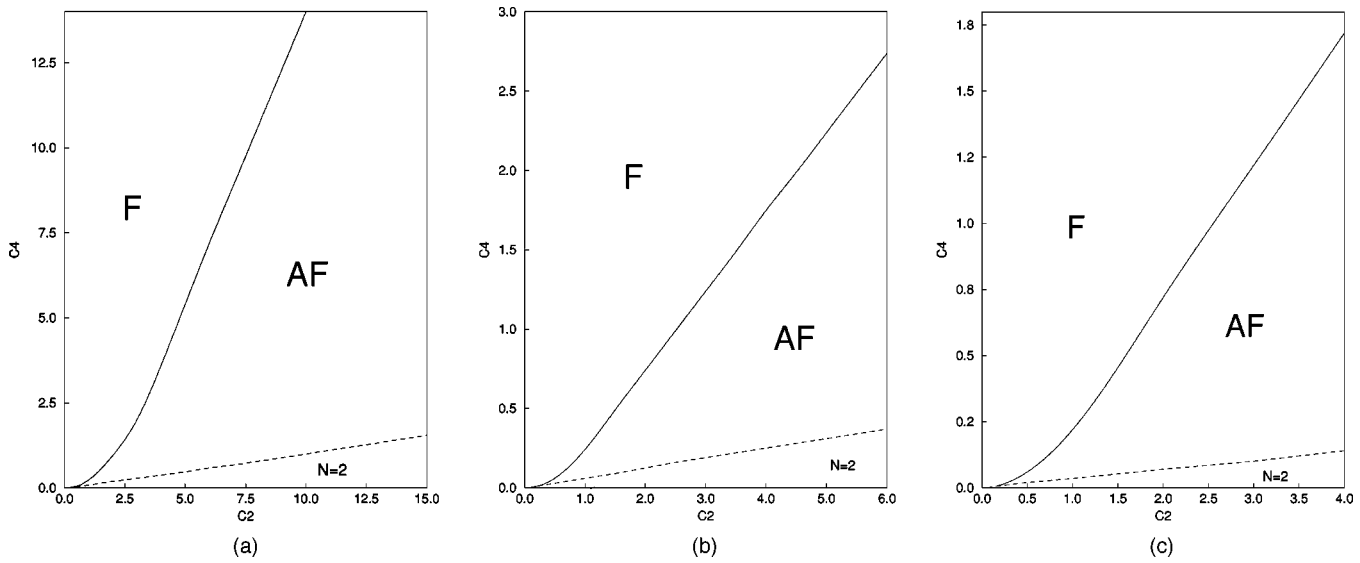

FIG. 4. The phase diagrams in (a) $d=2$, (b) $d=3$, and (c) $d=4$. The antiferromagnetic phase is found below the solid line. The lower region below the dashed line is the phase (1,2). The higher N phases are not shown.

$$S[\varphi(x)]=\sum_x \left\{ -\frac{1}{2}\varphi(x)\left[A\varphi(x)+\sum_\mu (B[\varphi(x+e_\mu)+\varphi(x-e_\mu)]+C[\varphi(x+2e_\mu)+\varphi(x-2e\mu)]+D[\varphi(x+3e_\mu)\right.\right.$$
$$+\varphi(x-3e_\mu)])+\sum_{\mu\neq\nu}(E[\varphi(x+e_\mu+e_\nu)+2\varphi(x+e_\mu-e_\nu)+\varphi(x-e_\mu-e_\nu)]+F[\varphi(x+2e_\mu+e_\nu)$$
$$+\varphi(x+2e_\mu-e_\nu)+\varphi(x-2e_\mu+e_\nu)+\varphi(x-2e_\mu-e_\nu)])+G\sum_{\mu\neq\nu\neq\rho}(\varphi(x+e_\mu+e_\nu+e_\rho)+3\varphi(x+e_\mu+e_\nu-e_\rho)$$
$$\left.\left.+3\varphi(x+e_\mu-e_\nu-e_\rho)+\varphi(x-e_\mu-e_\nu-e_\rho))\right]+\frac{m_L^2}{2}\varphi^2(x)+\frac{\lambda}{4}\varphi^4(x)\right\}, \tag{12}$$

where the coefficients A,B,C,D,E,F,G are defined by

$$A=-2d+(4d^2+2d)c_2-(8d^3+12d^2)c_4,$$
$$B=1-4dc_2+(12d^2+6d-3)c_4,$$
$$C=c_2-6dc_4,$$
$$D=c_4,$$
$$E=c_2-6dc_4,$$
$$F=3c_4,$$
$$G=c_4. \tag{13}$$

Only the ferromagnetic phase and the antiferromagnetic phase (1,2) were located (Fig. 4) by a numerical minimization of the action. The absolute minimum of the action is relativistic in the (1,2) antiferromagnetic phase, the nonrelativistic and anisotropic vacua lie higher as local minima.

IV. THE $c_4=0$ PHASES

We will determine the boundary of the para-, ferro-, and the (1,2) antiferromagnetic phases by means of the mean-field method. In the rest of this paper we will constrain ourselves to the case $c_4=0$. The explicit apparence of the cutoff makes the action with $c_4=0$ bounded from below.

We seek the vacuum in the form

$$\varphi(x)=\varphi_0+\varphi_1(-1)^{\sum_{\mu=1}^{d_{AF}} x^\mu}, \tag{14}$$

where φ_0 and φ_1 are variational parameters and d_{AF} is the number of antiferromagnetic directions. The action of the lattice Laplace operator on the vacuum is

$$\Box\varphi(x)=\sum_{\mu=1}^{d_{AF}}[\varphi(x+e_\mu)+\varphi(x-e_\mu)-2\varphi(x)]$$
$$=-4d_{AF}(\varphi(x)-\varphi_0), \tag{15}$$

which yields

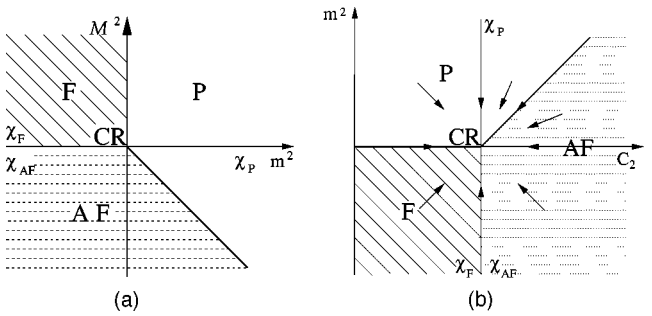

FIG. 5. The phase boundary between the paramagnetic (P), ferromagnetic (F) and the $N=2$ antiferromagnetic (AF) phase for $c_4=0$. The chiral symmetric regions χ_F, χ_{AF} and the critical point CR are on the phase boundary. (a) The plane $(m_L^2,\mathcal{M}_L^2)$. (b) The plane (c_2,m_L^2). The chiral line χ_P splits the paramagnetic phase into two parts. On the left of χ_P the particle of the restricted zone $\mathcal{B}_1$ is the lighter one. The particle of the zone $\mathcal{B}_{2^d}$ is the lighter one on the other side. The arrows show the possible continuum limits at the chiral invariant critical point, CR.

$$-\Box\mathcal{K}(\Box)\varphi(x)=\mathcal{M}_L^2(d_{AF},c_2)(\varphi(x)-\varphi_0), \tag{16}$$

where

$$\mathcal{M}_L^2(d_{AF},c_2)=4d_{AF}\mathcal{K}(-4d_{AF})=4d_{AF}(1-4d_{AF}c_2). \tag{17}$$

The minimization of the action density

$$s(\varphi_0^2,\varphi_1^2)=\frac{1}{2}m_L^2\varphi_0^2+\frac{1}{2}(m_L^2+\mathcal{M}_L^2)\varphi_1^2 + \frac{\lambda}{4}(\varphi_0^4+6\varphi_0^2\varphi_1^2+\varphi_1^4), \tag{18}$$

gives $d_{AF}=d$ and leads to the phase diagram in Fig. 5.

The $m_L^2<0$ case.

The equation

$$\mathcal{M}_L^2=0 \tag{19}$$

is a ferromagnetic-antiferromagnetic transition line. Clearly for $c_4=0$ there is no frustration in the system because the coupling constants C and E are both positive and then both of the ferromagnetic type. For $\mathcal{M}_L^2>0$ (i.e., $c_2<1/4d$) the B next to neighbor coupling is also positive and then the phase is ferromagnetic. For the saddle point we find $\varphi_0^2=-m_L^2/\lambda$, $\varphi_1^2=0$. Nevertheless it is important to notice that this phase is very different from the standard ferromagnetic phase of the theory without higher derivatives terms, where $C=E=0$ and $B>0$. In fact, as we will show later, in each phase of our model (the antiferromagnetic as well as the paramagnetic and the ferromagnetic ones) we find two kind of particles.

On the contrary for $\mathcal{M}_L^2<0$, B is negative (that is of the antiferromagnetic type) and the phase is antiferromagnetic. In this case the saddle point, is $\varphi_0^2=0$, $\varphi_1^2=-m_L^2+\mathcal{M}_L^2/\lambda$.

On the transition line $\mathcal{M}_L^2=0$, we have $B=0$. The absence of interactions between next neighbors causes the lattice to split into two different noninteracting (even and odd) sublattices. Approaching this line from the ferromagnetic side we have a ferromagnetic condensate of the same magnitude and sign in each of these sublattices. Approaching this line from the antiferromagnetic phase we have two ferromagnetic condensates of the same magnitude but opposite sign in the two sublattices. We will show later that on this line our theory is the superposition of two independent standard ferromagnetic ϕ^4 models.

The $m_L^2>0$ case.

The transition line between the paramagnetic and the antiferromagnetic phases is given by the equation

$$m_L^2+\mathcal{M}_L^2=0. \tag{20}$$

As before at the line $\mathcal{M}_L^2=0$, the next to neighbor coupling $B=0$. We will see later that on this line our model corresponds to the superposition of two standard paramagnetic ϕ^4 theories. If $\mathcal{M}_L^2>0$ then $B>0$ and the phase is paramagnetic as expected. For $-m_L^2<\mathcal{M}_L^2<0$, B is negative but the phase is still paramagnetic. The phase is antiferromagnetic when $\mathcal{M}_L^2<-m_L^2$.

V. THE ELEMENTARY EXCITATIONS

The quasiparticles of the mean-field approximation are given by the help of the free propagator. We will obtain the propagator in the different phases considered above. We start with

$$\langle\phi(x)\phi(y)\rangle=\int_{|p|\leqslant\pi}\frac{d^dp}{(2\pi)^d}e^{-ipx}G(p), \tag{21}$$

where

$$G^{-1}(p)=\tilde{m}_L^2+\hat{p}_\mu\hat{p}^\mu\mathcal{K}(-\hat{p}_\mu\hat{p}^\mu), \tag{22}$$

and

$$\hat{p}_\mu=2\sin\frac{p_\mu}{2}. \tag{23}$$

The mass parameter is given by

$$\tilde{m}_L^2=\begin{cases} m_L^2 & P,\\ -2m_L^2 & F,\\ -2m_L^2-3\mathcal{M}_L^2(d,c_2) & AF,\end{cases} \tag{24}$$

in the different phases. We write

$$G^{-1}(p)=\mathcal{P}^2(p)-c_2\mathcal{P}^4(p)+\tilde{m}_L^2, \tag{25}$$

with the notation

$$\mathcal{P}^2(p)=4\sum_\mu\sin^2\frac{p^\mu}{2}. \tag{26}$$

The excitations may take a momentum

$$P_\mu(\alpha)=\pi n_\mu(\alpha), \tag{27}$$

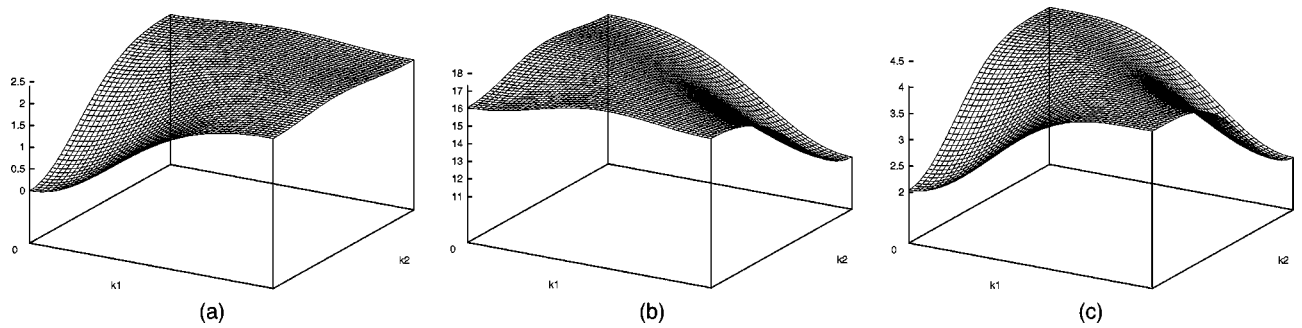

FIG. 6. The propagator in $d=2$ dimensions in the (a) ferro-, (b) antiferromagnetic phase and (c) at the phase boundary.

from the vacuum where $n_\mu(\alpha)=0$ or 1. The relation between the index $1\leqslant\alpha\leqslant 2^d$ and the vector $n_\mu(\alpha)$ is

$$\alpha=1+\sum_{\mu=1}^{d} n_\mu(\alpha)2^{\mu-1}. \tag{28}$$

It is then advantageous to split the

$$\mathcal{B}=\{k_\mu,\ |k_\mu|\leqslant\pi\} \tag{29}$$

Brillouin zone into 2^d restricted zones,

$$\mathcal{B}_\alpha=\left\{|k_\mu-P_\mu(\alpha)|\leqslant\frac{\pi}{2}\right\}. \tag{30}$$

The fluctuations around an extremum which is at the same time a minimum of the propagator are the particle like excitations. In this manner the single quantum field $\phi(x)$ might describe several particles at the same time. We will use the restricted zone notation in each phase and will see that only the particle modes survive in the continuum limit (see Fig. 6).

A. The extrema of the free propagator

In order to distinguish the particle like modes from other excitations we have to locate the extrema of the propagator. The derivative of the inverse propagator,

$$\frac{dG^{-1}}{dp_\sigma}=2\sin p_\sigma(1-2c_2\mathcal{P}^2(p)), \tag{31}$$

shows that the propagator has indeed 2^d extrema at the centers of the restricted Brillouin zones. The other extrema satisfy the equation

$$\mathcal{P}^2(p)=\frac{1}{2c_2}, \tag{32}$$

which are maxima. The inverse propagator takes the values

$$G^{-1}(P_\mu(\alpha))=\mathcal{M}_L^2(d(\alpha),c_2)+\tilde{m}_L^2, \tag{33}$$

at the center of the Brillouin restricted zones where the two variables function $\mathcal{M}_L^2$ is defined in Eq. (17) and

$$d(\alpha)=\sum_\mu n_\mu(\alpha) \tag{34}$$

is the number of dimensions with antiferromagnetic excitations.

The second derivative of the propagator is

$$\frac{\partial^2 G^{-1}}{\partial p_\sigma\partial p_\rho}=2\delta_{\rho\sigma}\cos p_\sigma(1-8c_2\mathcal{P}^2(p)) + 8\sin p_\sigma\sin p_\rho(12c_4\mathcal{P}^2(p)-c_2). \tag{35}$$

The Brillouin zone $\mathcal{B}_1$. We find

$$\left.\frac{\partial^2 G^{-1}}{\partial p_i^2}\right|_{p=P(1)}=2, \tag{36}$$

so the Bloch waves of the longest wavelength zone are always particle like.

The Brillouin zone $\mathcal{B}_{2^d}$.

$$\left.\frac{\partial^2 G^{-1}}{\partial p_i^2}\right|_{p=P(2^d)}=-2(1-8dc_2). \tag{37}$$

The right hand side is positive, and $\mathcal{B}_{2^d}$ describes particle like excitations in the region of the coupling constant space considered in the previous section.

The Brillouin zones $\mathcal{B}_\alpha$, $\alpha=2,\ldots,15$. We present here the case $\alpha=2$ only where $P_\mu(2)=(\pi,0,0,0)$,

$$\left.\frac{\partial^2 G^{-1}}{\partial p_1^2}\right|_{p=P(2)}=-2(1-8c_2+64c_4),$$

$$\left.\frac{\partial^2 G^{-1}}{\partial p_l^2}\right|_{p=P(2)}=2(1-8c_2+48c_4), \tag{38}$$

for $l=2,3,4$ and

$$\left.\frac{\partial^2 G^{-1}}{\partial p_\mu\partial p_\nu}\right|_{p=P(2)}=0 \tag{39}$$

for $\mu\neq\nu$. The other zones yield similar result and they contain no extrema but saddle points only.

TABLE I. The parameters of the propagator for $\mathcal{B}_\alpha$, $\alpha=1$ and 16.

Phase	$\tilde{m}_L^2(1)$	$\tilde{m}_L^2(16)$	$Z(1)$	$Z(16)$
P	m_L^2	$m_L^2+\mathcal{M}_L^2$	1	$-1+32c_2$
F	$-2m_L^2$	$-2m_L^2+\mathcal{M}_L^2$	1	$-1+32c_2$
AF	$-2m_L^2-3\mathcal{M}_L^2$	$-2m_L^2-2\mathcal{M}_L^2$	1	$-1+32c_2$

Thus one finds two particle modes in the phases considered. The other 14 reduced Brillouin zones have excitations which are nonparticle type.

B. The continuum limit

In order remove the 14 unusual excitations found above we take the continuum limit, $a\to 0$. This is quite a simple procedure in the mean-field approximation where the quantum fluctuations are kept noninteracting. We keep the mass parameter m^2 of the Lagrangian cutoff independent in this approximation so $m_L^2=O(a^2)$.

The propagator

$$G^{-1}(p)=\tilde{m}_L^2+\mathcal{P}^2(p)-c_2\mathcal{P}^4(p), \tag{40}$$

yields

$$\lim_{p\to 0} G_\alpha^{-1}(p)=\tilde{m}_L^2(\alpha)+Z(\alpha)p^2+O(p^4), \tag{41}$$

for the fluctuations in $\mathcal{B}_1$ and $\mathcal{B}_{16}$. The mass and the wave function renormalization constant are given in Table I for $\alpha=1$ and 16.

Notice that the finiteness of the mass in $\mathcal{B}_{16}$ requires a tree-level renormalization of c_2, such that $\mathcal{M}_L^2(4,c_2)=O(a^2)$. The continuum limit of the mean-field solution is achieved at the critical point CR of Fig. 5.

In the other restricted Brillouin zones in each phase we get

$$\lim_{p\to 0} G^{-1}(P(\alpha)+p)=p^2[1-8c_2d(\alpha)]-p'^2[1-8c_2d(\alpha)]$$
$$+4d(\alpha)-16c_2d^2(\alpha)+\tilde{M}^2(\alpha), \tag{42}$$

where $d(\alpha)$ is given by Eq. (34) and $p'=P(16)-p$. The particular form of $\tilde{M}^2(\alpha)$ depends on the phase and diverges as $O(a^{-2})$ when the masses in the $\alpha=1$ and $\alpha=16$ regions are kept finite.

The mass spectrum. We define the chiral lines χ_P, χ_F and χ_{AF} as the lines where the masses of the two particles $\tilde{m}_L^2(1)$ and $\tilde{m}_L^2(16)$ are degenerate in each of the three phases considered above. These lines are actually given by the equation $\mathcal{M}_L^2=0$ [see Fig. 5(b)]. As this line for $m_L^2<0$ is also the F-AF phase transition line, χ_F and χ_{AF} are actually one and the same line. The energy density and the particle content approaching this line from the two sides are the same. It is worth to remind that in this case the even and odd sublattices are decoupled and that the difference between the upper and lower side of this line lies on the sign of the ferromagnetic condensate on each of these sublattices.

The particle of the restricted zone $\mathcal{B}_1$ is the lighter one in the ferromagnetic phase and on the left of the chiral line χ_P in the paramagnetic phase. The staggered excitations of $\mathcal{B}_{2^d}$ are the lighter ones in the antiferromagnetic phase and on the right of χ_P. The excitations of the restricted zone $\mathcal{B}_{2^d}$ are always massless along the transition line $P-AF$.

C. The momentum conservation

The momentum is not conserved in the antiferromagnetic phase because the particles may exchange momentum with the inhomogeneous vacuum. One can recover the momentum conservation by the introduction of the momentum

$$p_\mu\to p_{AF\mu}=p_\mu(\mathrm{mod}\,\pi), \tag{43}$$

where the quanta of the momentum which can be borrowed from the vacuum is removed. Whenever this happens the particle type changes. The simultaneous shift of all components, $p\to p+P(2^d)$, corresponds to the exchange of the two particles, $1\leftrightarrow 2^d$.

VI. THE SYMMETRIES

The phase structure and the order parameter of the model is quite involved so it is all the more important to find the symmetries relevant to the phase transitions. We can identify two kind of symmetries, one which is realized at certain points only of the phase boundary and others which distinguish the different phases.

A. Chiral symmetry

There are two particles in the model so one expects that the theory where the two particle species become symmetrical might be special. The transformation

$$\chi:\quad \phi(x)\to(-1)^{\sum_\mu x^\mu}\phi(x), \tag{44}$$

which amounts to the shift

$$p_\mu\to p_\mu+P_\mu(2^d) \tag{45}$$

connecting the particle species will be called chiral transformation [19]. It always leaves the ultralocal even potential energy invariant. The propagator and with it the kinetic energy changes as

$$\begin{aligned} G^{-1}(p)&=\mathcal{P}^2(p)-c_2\mathcal{P}^4(p)+\tilde{m}_L^2\\ &\to 1-\mathcal{P}^2(p)-c_2[1-\mathcal{P}^2(p)]^2+\tilde{m}_L^2\\ &=(-1+8dc_2)\mathcal{P}^2(p)+(-c_2)\mathcal{P}^4(p)\\ &\quad+\mathcal{M}_L^2(d,c_2)+\tilde{m}_L^2. \end{aligned} \tag{46}$$

The theory which is invariant under χ,

$$c_2=\frac{1}{4d}, \quad c_4=0, \tag{47}$$

will be called chiral symmetrical. Note that mass parameter of the kinetic energy is vanishing, $\mathcal{M}_L^2(d,c_2)=0$ and the two particle species are degenerate in such a theory.

The operator $\mathcal{P}_\pm=\frac{1}{2}(1\pm\chi)$ projects on the fields belonging to the even or odd sublattices,

$$\mathcal{P}_\pm\phi_\pm=\phi_\pm . \tag{48}$$

The kinetic energy couples ϕ_+ and ϕ_- in general. Since the transformation (44) acts as

$$\phi_\pm\to\pm\phi_\pm , \tag{49}$$

the fields ϕ_+ and ϕ_- decouple in the chiral invariant theory. This decoupling gives another insight into the dynamics of the phase transitions. The chiral theory contains two independent and equivalent ϕ^4 theories. If they are in the symmetry broken phase then their condensate has the same absolute magnitude. The relative phase is undetermined and will be the result of the microscopic differences between the fluctuations of the two fields, in a manner similar to a spontaneous symmetry breaking. The ferromagnetic phase is realized when the sign of the condensates agree. The sign is the opposite in the antiferromagnetic case. The spontaneous symmetry breaking is the result of the infrared modes in the independent theories. In case when the sign of the condensate happens to be different then the resulting vacuum of the original theory which contains both sublattices has an ultraviolet condensate. In this manner the original, infrared mechanism appears in the ultraviolet and generates dynamical symmetry breaking for the observables of the complete lattice.

B. Chiral bosons

The origin of the chiral symmetry becomes clearer by introducing the hypercube variables $x^\mu=2y^\mu+n^\mu$ where n^μ labels the different sites of the elementary cell of the (1,2) antiferromagnetic vacuum and the chiral fields [20]

$$\phi_n(y)=\phi_\alpha(y)=\phi(2y+n(\alpha)). \tag{50}$$

We need the linear superpositions [21]

$$\tilde{\phi}_\alpha(y)=A_{\alpha\beta}\phi_\beta(y), \tag{51}$$

where the matrix

$$A_{\alpha\beta}=2^{-d/2}(-1)^{n(\alpha)\cdot n(\beta)} \tag{52}$$

performs the Z_2 Fourier transformation in the elementary cell. Since

$$(A^2)_{n,n'}=2^{-d}\sum_m (-1)^{m\cdot(n+n')}=\delta_{n,n'}, \tag{53}$$

the inverse Fourier transformation is

$$\phi_\alpha(y)=A_{\alpha\beta}\tilde{\phi}_\beta(y). \tag{54}$$

The chiral transformation is diagonal on the chiral field basis,

$$\chi: \quad \phi_\alpha(y)\to\chi(n(\alpha))\phi_\alpha(y), \tag{55}$$

where

$$\chi(n)=(-1)^{\sum_\mu n^\mu}=(-1)^{E(0)\cdot n}. \tag{56}$$

The vector of the last expression is defined as

$$E_\mu(k)=\begin{cases}1 & k\leqslant\mu,\\ 0 & \text{otherwise.}\end{cases} \tag{57}$$

C. Space-time inversions

The space-time inversions will serve two purposes: On the one hand, they demonstrate the formal similarity between the field $\phi_\alpha(y)$ and the chiral fermions. On the other hand, they are the symmetries which distinguish the ferromagnetic and the antiferromagnetic phase. The inversion I_ν of the coordinate

$$I_\nu: \quad x^\mu\to I_\nu x^\mu=(-1)^{\delta_{\mu\nu}}x^\mu, \tag{58}$$

is defined in such a manner that it maps the elementary cells into each other. It flips the μ-th components of the elementary cell vector n_μ,

$$I_\mu: \quad \phi(y)\to U_\mu\phi(I_\mu y), \tag{59}$$

where the matrix U_μ acting on the elementary cell is defined as

$$(U_\mu)_{n,m}=\begin{cases}1 & \text{if } n_\nu+m_\nu=\delta_{\mu,\nu}(\text{mod}2),\\ 0 & \text{otherwise.}\end{cases} \tag{60}$$

The space inversion, $P=\Pi_{l=2}^d I_l$, is

$$P: \quad \phi(y)\to U_P\phi(Py), \tag{61}$$

where

$$(U_P)_{n,m}=\left(\prod_{l=2}^d U_l\right)_{n,m}=\begin{cases}1 & \text{if } n+m=E(1)(\text{mod}2),\\ 0 & \text{otherwise.}\end{cases} \tag{62}$$

The field $U_P\phi(y)$ will be called the P-helicity partner of $\phi(y)$. The combined effect of the time inversion $T=I_1$ and the space inversion is represented by

$$PT: \quad \phi(y)\to U_{PT}\phi(PTy), \tag{63}$$

$$(U_{PT})_{n,m}=\left(\prod_\mu U_\mu\right)_{n,m}=\begin{cases}1 & \text{if } n+m=E(0)(\text{mod}2),\\ 0 & \text{otherwise.}\end{cases} \tag{64}$$

$U_{PT}\phi(y)$ will be called the PT-helicity partner of $\phi(y)$. Finally we define ρ as

$$\rho=\begin{cases} P & \text{even } d, \\ PT & \text{odd } d, \end{cases} \tag{65}$$

which maps the fields of the two sublattices, ϕ_+ and ϕ_- into each other in a specific manner.

We found that the chiral transformation is diagonal and the space-time inversions are nondiagonal in the chiral field basis. The situation is just the opposite after a Fourier transformation. First we show that the Fourier transformed fields are eigenvectors of the space-time inversions. $\tilde{U}_\mu$ which represents I_μ on the Fourier transformed elementary cell is given by $\tilde{U}_\mu A=AU_\mu$, what yields

$$\begin{aligned}(\tilde{U}_P)_{n,n'}&=(AU_PA)_{n,n'}\\ &=2^{-d}\sum_m (-1)^{m\cdot(n+n')+n\cdot E(1)}\\ &=\delta_{n,n'}(-1)^{n\cdot E(1)}\\ &=\delta_{n,n'}(-1)^{\sum_{l=2^n l}^d}.\end{aligned} \tag{66}$$

In a similar manner we have

$$(\tilde{U}_{PT})_{n,n'}=\delta_{n,n'}(-1)^{\sum_{\mu=1}^d n_\mu}=\delta_{n,n'}\chi(n). \tag{67}$$

Thus the Fourier transformed fields have well defined space and time inversion parities,

$$\sigma_P=(-1)^{\sum_{l=2^n l}^d},\quad \sigma_T=(-1)^{n^1}. \tag{68}$$

On the contrary, the chiral transformation becomes nondiagonal after a Fourier transformation,

$$\chi:\quad \tilde{\phi}_\alpha(y)\to\tilde{\phi}_{\bar{\alpha}}(y), \tag{69}$$

with $\bar{\alpha}=2^d+1-\alpha$. The corresponding transformation of the vector index $n_\mu(\alpha)$ is

$$\chi:\quad n\to\bar{n}=n+E(0)(\mathrm{mod}2). \tag{70}$$

D. Bosonic chiral theory

It is worthwhile to compare our result with the fermionic case.

Particle species. The naive fermion theory has 2^d species in lattice regularization which is just the number of restricted Brillouin zones in the antiferromagnetic phase (1,2). Out of the 2^d restricted Brillouin zones only two contain particle modes for small c_4. The helicity, the projection of the angular momentum on the momentum of a scalar particle is identically vanishing. Nevertheless one can construct a pair of scalar fields $\phi_\pm(x)=\phi_s(x)\pm\phi_{ps}(x)$, which are exchanged under space inversion by the help of a scalar and a pseudoscalar field, $\phi_s(x)$, $\phi_{ps}(x)$, respectively. The chiral spinors are exchanged by the space inversion, $U_P=i\gamma_0$. By analogy we may call $\phi_\pm(x)$ and $\phi_\alpha(y)$ chiral fields. The excitations around $p=P(1)$ and $P(16)$ of the Brillouin zone correspond to the slowly varying fields $\phi_s(x)$ and $\phi_{ps}(x)$, respectively. Note that the projection of the angular momentum on the momentum is the same, 0, for all members of the $O(d)$ multiplet of the chiral scalar particle as for the $(1+1)$-dimensional fermions.

Chiral symmetry. The chiral spinors decouple in the massless fermionic theory as our chiral boson fields do at the theory (47). The analogue of the discrete chiral transformation, $\psi\to\gamma_5\psi$, is $\phi\to\chi\phi$, given by Eq. (44). The standard representation for the Dirac bispinors provides fields with well defined parity similar to the Fourier transformed chiral fields of the scalar model.

Chiral charge. The chiral charge of a chiral spinor is its eigenvalue for γ_5. The sum of the chiral charge is zero for the naive fermions on the lattice. The chiral charge of the scalar modes on the even or the odd sublattices is $+1$ or -1, respectively. Thus the total chiral charge is vanishing in our model as long as there are as many degrees of freedom on the even as on the odd sublattice.

Chiral particles. The chiral fermions represent a serious problem in lattice regularization because the theory with a single chiral fermion is not covariant under space inversion. The realization of this condition meets difficulties in the usual lattice theories [22]. There is more flexibility in the scalar model where we might as well use the symmetrical or the anti-symmetrical combination of the two particle modes in $\mathcal{B}_1$ and $\mathcal{B}_{2^d}$ for the chiral symmetrical theory. In fact, these modes are degenerate and decouple. Such a combinations correspond to the fields $\phi_\pm$ constructed in Eq. (48). Since these fields have no interactions between themselves one of them can be set to zero. The resulting model which exists only at the chiral point contains a single particle with nonvanishing chiral charge and a freely adjustable mass and coupling constant,

$$\mathcal{L}_\pm=\frac{1}{2}(\partial_\mu\phi_\pm)^2+\frac{m^2}{2}\phi_\pm^2+\frac{\lambda}{4}\phi_\pm^4, \tag{71}$$

in the continuum limit of the mean-field approximation.

The no-go theorem, [22], about the impossibility of having a single fermion with nonvanishing chiral charge has topological origin. The nontrivial elementary cell of the antiferromagnetic phase which becomes small in the continuum limit offers the possibility of avoiding the usual transformation rules with respect the space-inversions and thereby circumvents the problem at least for bosons. The differences of the physical properties of a chiral and an ordinary boson with well defined parity will only be seen after coupling the chiral boson to other particles.

When the theory with broken chiral symmetry is considered then the chiral fields $\phi_\pm$ are coupled. The low energy elementary excitations are made of the slowly varying fields $\phi_\pm$ as

$$\tilde{\phi}_\pm=\phi_+\pm\phi_-. \tag{72}$$

TABLE II. The symmetry of different regions of the coupling constant space. A symmetry can be manifest (√), broken explicitly (E), spontaneously by the IR modes (S), or dynamically by the UV modes (D).

Phase	χ	ρ	γ
P	E	√	√
F	E	√	S
AF	E	D	D
CR	√	√	√
χ_P	√	√	√
χ_F	√	√	S
χ_{AF}	√	D	D

The ρ parity of the field $\tilde{\phi}_\pm$ is ± 1 and it belongs to the zone $\mathcal{B}_1$ and $\mathcal{B}_{16}$. The effective theory obtained on the tree level, Eq. (18), is

$$L=\frac{1}{2}(\partial_\mu\tilde{\phi}_+)^2+\frac{1}{2}(\partial_\mu\tilde{\phi}_-)^2+\frac{m_+^2}{2}\tilde{\phi}_+^2+\frac{m_-^2}{2}\tilde{\phi}_-^2 + \frac{\lambda}{4}(\tilde{\phi}_+^4+\tilde{\phi}_-^4+6\tilde{\phi}_+^2\tilde{\phi}_-^2), \tag{73}$$

for low enough energy where the further influence of the higher order derivatives on the propagator is negligible.

E. The symmetries of the phase diagram

For the more complete characterization of the symmetries of the model we finally introduce the discrete analogue of the charge conjugation to our real field,

$$\gamma: \quad \phi(x)\rightarrow -\phi(x). \tag{74}$$

The symmetries of different regions of the coupling constant space (m_L^2, c_2) is shown for $c_4=0$ in Table II. One can see that the ferromagnetic condensate is detectable by the internal space order parameter only. The dynamical breakdown of the space inversion symmetry in the vacuum is characteristic of the antiferromagnetic phase. In agreement with this remark the particle scattering off such a vacuum may borrow the momentum $P(2^d)$ and change its parity.

VII. CONCLUSION

We showed an interplay between the symmetry breaking patterns in the internal and the external space realized by the higher dimensional pieces of the kinetic energy term of the action of a ϕ^4 theory. The strongly distance dependent interactions described by these pieces generate nontrivial elementary cells in the vacuum and render the dynamics of the system somewhat similar to solid state physics.

A complex phase structure was found with a number of commensurate incommensurate transitions. Concerning the elementary excitations there are two particle modes in the vicinity of the antiferromagnetic (1,2) phase, the analogues of the acoustic and optical phonons of the solid states because they correspond to the in phase and the out of phase oscillations in the elementary cell. The emergence of the nonhomogeneous condensate of the phase (1,2) reduces the translation invariance into translation by even number of the lattice spacing. Nevertheless no Goldstone bosons appear. This is because the condensate is at the cutoff scale where the continuous translation symmetry is broken by the regularization.

The space inversion exchanges the two particles of the theory. This opens the possibility of constructing chiral bosons on the lattice for such a choice of the coupling constants where these two particles decouple. We showed that the dynamical breaking of the space inversion symmetry is characteristic to the formation of the nontrivial elementary cells of the antiferromagnetic phase.

We believe that the phenomena mentioned in the framework of the scalar ϕ^4 model are generic and can be found in any bosonic model. A theoretical test of such a model as a more realistic effective theory is the possibility of removing the length scale of the elementary cell of the vacuum in order to suppress the non-unitary processes related to the creation of the lattice defects [19,23,24]. The period length of the vacuum can be sent to zero in the one-loop approximation [25]. It remains to be seen if this result generalizes to higher loop order.

ACKNOWLEDGMENTS

J.P. thanks Jochen and Werner Fingberg for illuminating discussions.

[1] K. Wilson and J. Kogut, Phys. Rep., Phys. Lett. **C12**, 75 (1974); K. Wilson, Rev. Mod. Phys. **47**, 773 (1975).
[2] W.A. Bardeen, C.N. Leung, and S.T. Love, Nucl. Phys. **B323**, 493 (1989); C.N. Leung, S.T. Love, and W.A. Bardeen, *ibid.* **B273**, 649 (1986).
[3] P.I. Fomin, V.P. Gusynin, V.A. Miransky, and Yu.A. Sitenko, Riv. Nuovo Cimento **6**, 5 (1983).
[4] S.B. Liao and J. Polonyi, Phys. Rev. D **51**, 4474 (1995).
[5] V. Branchina and J. Polonyi, Nucl. Phys. **B433**, 99 (1995).
[6] V. Branchina and J. Polonyi, ''Mini-instantons in SU(2) Gauge Theory,'' hep-th/9606160.
[7] J. Alexandre, V. Branchina, and J. Polonyi, Phys. Rev. D **58**, 016002 (1998).
[8] Y. Nambu and G. Jona-Lasinio, Phys. Rev. **122**, 345 (1961).
[9] G. Grüner, *Density Waves in Solids* (Addison-Wesley, Readwood City, CA, 1994).
[10] S. Coleman, *Aspects of Symmetry* (Cambridge University Press, Cambridge, England, 1985); J. Collins, *Renormalization* (Cambridge University Press, Cambridge, England, 1984).
[11] J. Polonyi, in *Quark-Gluon Plasma*, edited by R. Hwa (World Scientific, Singapore, 1988).
[12] J.L. Alonso *et al.*, ''Non-classical exponents in the d=4 Ising

model with two couplings,'' e-Print Archive: hep-lat/9503016; I. Campos, L.A. Fernández, and A. Tarancon, Phys. Rev. D **55**, 2965 (1997); J.L. Alonso *et al.*, Nucl. Phys. B (Proc. Suppl.) **47**, 767 (1996); H.G. Ballesteros, L.A. Fernández, V. Martin-Mayor, and Munoz Sudupe, Phys. Lett. B **378**, 207 (1996); Nucl. Phys. **B483**, 707 (1997); Nucl. Phys. B (Proc. Suppl.) **53**, 686 (1997); H.G. Ballesteros *et al.*, Phys. Rev. D **55**, 5067 (1997).

[13] G. Parisi and J.J. Ruiz-Lorenzo, J. Phys. A **28**, L395 (1995).

[14] S. Caracciolo and S. Patarnello, Phys. Lett. A **126**, 233 (1988); M. Bernashi *et al.*, Phys. Lett. B **231**, 157 (1989); L.A. Fernandez *et al.*, *ibid.* **217**, 314 (1989); R.V. Gavai and F. Karsch, Phys. Rev. B **46**, 944 (1992); S.J. Ferreira and A.D. Sokal, *ibid.* **51**, 6727 (1995).

[15] Y. Shamir, Phys. Rev. D **57**, 132 (1998).

[16] P. Bak, Rep. Prog. Phys. **45**, 587 (1982); R.B. Griffiths, in *Fundamental Problems in Statistical Mechanics, VII*, edited by H. van Beijeren (Elsevier Science, Amsterdam, 1990).

[17] Y.I. Frenkel and T. Kontorowa, Zh. Eksp. Teor. Fiz. **8**, 1340 (1938); F.C. Frank and J.H. Van der Merwe, Proc. R. Soc. London **A198**, 205 (1949); **A198**, 216 (1949).

[18] W.L. McMillan, Phys. Rev. B **4**, 1496 (1976); V.L. Pokrovcky and A.L. Talapov, Zh. Éksp. Teor. Fiz. **75**, 1151 (1978) [Sov. Phys. JETP **48**, 579 (1978)]; A.D. Novaco, Phys. Rev. B **22**, 1645 (1980); T. Janssen and J.A. Tjom, *ibid.* **25**, 3767 (1982).

[19] J. Polonyi, in the proceedings of the Workshop on ''Quark Confinement and Hadron Spectroscopy II,'' Como, Italy, 1996, hep-lat/9610030.

[20] H. Kluberg-Stern, A. Morel, O. Napoly, and B. Petersson, Nucl. Phys. **B220**, 447 (1983).

[21] H.S. Sharatchandra, H.J. Thun, and P. Weisz, Nucl. Phys. **B192**, 205 (1981).

[22] H.B. Nielsen and M. Ninomiya, Nucl. Phys. **B185**, 20 (1981).

[23] A. Pais and G.E. Uhlenbeck, Phys. Rev. **79**, 145 (1950); T.D. Lee and G.C. Wick, Nucl. Phys. **B9**, 209 (1969); Phys. Rev. D **2**, 1033 (1970); Chung-I Tan and Zai-Xin Xu, *ibid.* **30**, 455 (1984); C. Liu, K. Jansen, and J. Kuti, Nucl. Phys. B (Proc. Suppl.) **34**, 635 (1994); **42**, 630 (1995).

[24] J. Fingberg and J. Polonyi, Nucl. Phys. **B486**, 315 (1997).

[25] V. Branchina, H. Mohrbach, and J. Polonyi, Phys. Rev. D **60**, 045007 (1999).